Atmos. Chem. Phys., 22, 11347–11358, 2022
https://doi.org/10.5194/acp-22-11347-2022

Atmospheric Chemistry and Physics
Open Access
EGU

The positive effect of formaldehyde on the photocatalytic renoxification of nitrate on TiO_2 particles

Yuhan Liu, Xuejiao Wang, Jing Shang, Weiwei Xu, Mengshuang Sheng, and Chunxiang Ye

State Key Joint Laboratory of Environmental Simulation and Pollution Control, College of Environmental Sciences and Engineering, Peking University, 5 Yiheyuan Road, Beijing 100871, PR China

Correspondence: Jing Shang (shangjing@pku.edu.cn)

Received: 5 January 2022 – Discussion started: 27 January 2022
Revised: 4 August 2022 – Accepted: 11 August 2022 – Published: 5 September 2022

Abstract. Renoxification is the process of recycling NO_3^- / HNO_3 into NO_x under illumination and is mostly ascribed to the photolysis of nitrate. TiO_2, a typical mineral dust component, is able to play a photocatalytic role in the renoxification process due to the formation of NO_3 radicals; we define this process as "photocatalytic renoxification". Formaldehyde (HCHO), the most abundant carbonyl compound in the atmosphere, may participate in the renoxification of nitrate-doped TiO_2 particles. In this study, we established a 400 L environmental chamber reaction system capable of controlling 0.8 %–70 % relative humidity at 293 K with the presence of 1 or 9 ppm HCHO and 4 wt % nitrate-doped TiO_2. The direct photolyses of both nitrate and NO_3 radicals were excluded by adjusting the illumination wavelength so as to explore the effect of HCHO on the "photocatalytic renoxification". It was found that NO_x concentrations can reach up to more than 100 ppb for nitrate-doped TiO_2 particles, while almost no NO_x was generated in the absence of HCHO. Nitrate type, relative humidity and HCHO concentration were found to influence NO_x release. It was suggested that substantial amounts of NO_x were produced via the NO_3^-–NO_3•–HNO_3–NO_x pathway, where TiO_2 worked for converting "NO_3^-" to "NO_3• ", that HCHO participated in the transformation of "NO_3• " to "HNO_3" through hydrogen abstraction, and that "HNO_3" photolysis answered for mass NOx release. So, HCHO played a significant role in this "photocatalytic renoxification" process. These results were found based on simplified mimics for atmospheric mineral dust under specific experimental conditions, which might deviate from the real situation but illustrated the potential of HCHO to influence nitrate renoxification in the atmosphere. Our proposed reaction mechanism by which HCHO promotes photocatalytic renoxification is helpful for deeply understanding atmospheric photochemical processes and nitrogen cycling and could be considered for better fitting atmospheric model simulations with field observations in some specific scenarios.

1 Introduction

The levels of ozone (O_3) and hydroxyl radicals (•OH) in the troposphere can be promoted by nitrogen oxides ($NO_x = NO + NO_2$), such that NO_x plays an important role in the formation of secondary aerosols and atmospheric oxidants (Platt et al., 1980; Stemmler et al., 2006; Harris et al., 1982; Finlayson-Pitts and Pitts, 1999). NO_x can be converted into nitric acid (HNO_3) and nitrate (NO_3^-) through a series of oxidation and hydrolysis reactions and is eventually removed from the atmosphere through subsequent wet or dry deposition (Dentener and Crutzen, 1993; Goodman et al., 2001; Monge et al., 2010; Bedjanian and El Zein, 2012). However, comparisons of observations and modeling results for the marine boundary layer, land, and free troposphere (Read et al., 2008; Lee et al., 2009; Seltzer et al., 2015) have shown an underestimation of HNO_3 or NO_3^- content, NO_x abundance, and NO_x / HNO_3 ratios, indicating the presence of a new, rapid NO_x circulation pathway (Ye et al., 2016b; Reed et al., 2017). Some researchers have suggested that deposited NO_3^- and HNO_3 can be recycled back to gas-phase NO_x under illumination via the renoxification process (Schuttlefield et al., 2008; Romer et al., 2018; Bao et al., 2020; Shi et al., 2021).

Photolytic renoxification occurs under light with a wavelength of < 350 nm through the photolysis of NO_3^- / HNO_3 adsorbed on the solid surface to generate NO_x. Notably, the photolysis of NO_3^- / HNO_3 is reported to occur at least 2 orders of magnitude faster on different solid surfaces (natural or artificial) or on aerosols than in the gas phase (Ye et al., 2016a; Zhou et al., 2003; Baergen and Donaldson, 2013). Several recent studies have shown that renoxification has important atmospheric significance (Deng et al., 2010; Kasibhatla et al., 2018; Romer et al., 2018; Alexander et al., 2020), providing the atmosphere with a new source of photochemically reactive nitrogen species, i.e., HONO or NO_x, resulting in the production of more photooxidants such as O_3 or •OH (Ye et al., 2017), which further oxidize volatile organic compounds (VOCs), leading to the formation of more chromophores and thereby affecting the photochemical process (Bao et al., 2020).

Renoxification processes have recently been observed on different types of atmospheric particles, such as urban grime and mineral dust (Ninneman et al., 2020; Bao et al., 2018; Baergen and Donaldson, 2013; Ndour et al., 2009). Atmospheric titanium dioxide (TiO_2) is mainly derived from windblown mineral dust, with mass mixing ratios ranging from 0.1 % to 10 % (Chen et al., 2012). TiO_2 is widely used in industrial processes and building exteriors for its favorable physical and chemical properties. Titanium and nitrate ions have been found to coexist in atmospheric particulates in different regions worldwide (Sun et al., 2005; Liu et al., 2005; Yang et al., 2011; Kim et al., 2012), and the NO_3^- / ($NO_3^- + TiO_2$) mass percentage of total suspended particulate matter (TSP) during dust storms can be lower than 20 % (Sun et al., 2005). In this case, nitrate-coated TiO_2 (NO_3^-–TiO_2) aerosols containing TiO_2 as the main body can, to some extent, be used to represent the real situation under sandstorms. TiO_2 is a semiconductor metal oxide that can facilitate the photolysis of nitrate and the release of NO_x due to its photocatalytic activity (Ndour et al., 2009; Chen et al., 2012; Verbruggen, 2015; Schwartz-Narbonne et al., 2019). Under UV light, TiO_2 generates electron-hole pairs in the conduction and valence bands, respectively (Linsebigler et al., 1995). Nitrate ions adsorbed at the oxide surface react with the photogenerated holes (h^+) to form nitrate radicals (NO_3•), which are subsequently photolyzed to NO_x, mainly under visible illumination (Schuttlefield et al., 2008; George et al., 2015; Schwartz-Narbonne et al., 2019). Thus, the renoxification of NO_3^- is faster on TiO_2 than on other oxides in mineral dust aerosols such as SiO_2 or Al_2O_3 (Lesko et al., 2015; Ma et al., 2021). In this study, we refer to renoxification involving h^+ and NO_3^- as photocatalytic renoxification based on the photocatalytic properties of TiO_2.

Many previous studies have focused mainly on particulate nitrate–NO_x photochemical cycling reactions despite the potential impact of other reactant gases in the atmosphere. Formaldehyde (HCHO), the most abundant carbonyl compound in the atmosphere, can reach as high as 0.4 ppm in some specific situations (particularly in some indoor air or in cities with high traffic density) (Wilbourn et al., 1995; Salthammer, 2019). HCHO can react with NO_3• at night via hydrogen abstraction reactions to form HNO_3 (Atkinson, 1991). Our previous study showed that the degradation rate of HCHO was faster on NO_3^-–TiO_2 aerosols than on TiO_2 particles, perhaps as a result of HCHO oxidation by NO_3• (Shang et al., 2017). To date, no studies have reported the effect of HCHO on photocatalytic renoxification. Adsorbed HCHO would react with NO_3• generated on the NO_3^-–TiO_2 aerosol surface, thus altering the surface nitrogenous species and renoxification process. The present study is the first to explore the combined effect of HCHO and photocatalytic TiO_2 particles on the renoxification of nitrate. The wavelengths of the light sources were adjusted to exclude photolytic renoxification while making photocatalytic renoxification available for better elucidating the reaction mechanism. We investigated the effects of various influential factors – including nitrate type, nitrate content, RH, and initial HCHO concentration – to understand the atmospheric renoxification of nitrate in greater detail.

2 Methods

2.1 Environmental chamber setup

Details of the experimental apparatus and protocol used in the current study have been previously described (Shang et al., 2017). Briefly, the main body of the environmental chamber is a 400 L polyvinyl fluoride (PVF) bag filled with synthetic air (high purity N_2 (99.999 %) mixed with high purity O_2 (99.999 %) with a ratio of 79:21 by volume; Beijing Huatong Jingke Gas Chemical Co.). The chamber is capable of temperature (~ 293 K) and relative humidity (0.8 %–70 %) control using a water bubbler and air conditioners, respectively. The chamber is equipped with two light sources, both with a central wavelength of 365 nm. One is a set of 36 W tube lamps with a main spectrum of 320–400 nm and a small amount of 480–600 nm visible light (Fig. S1a). The other is a set of 12 W LED lamps with a narrow main spectrum of 350–390 nm (Fig. S1b). The light intensities for the tube and LED lamp at 365 nm were 300 and 200 $\mu W\,cm^{-2}$, respectively, as measured in the middle of the chamber. NO_x concentrations at the outlet of the chamber were monitored by a chemiluminescence NO_x analyzer (ECOTECH, EC9841B). HCHO was generated by thermolysis of paraformaldehyde at 70 °C and detected via an acetyl acetone spectrophotometric method using a UV–Vis spectrophotometer (PERSEE, T6) or a fluorescence spectrophotometer (THERMO, Lumina), depending on different initial HCHO concentrations. The particle size distribution was measured by a scanning nanoparticle spectrometer (HCT, SNPS-20). Electron spin resonance (Nuohai Life Science, MiniScope MS 5000) was used to measure •OH on the surface of the particles. A 5,5-dimethl-1-pyrroline-N-oxide (DPMO, Enzo) was used as the

capture agent. Fifty µL particle-containing suspension mixed with 50 µL DMPO (concentration of 200 µM) was loaded in a 1 mm capillary. Four 365 nm LED lamps were placed side by side, vertically, at a distance of about 1 cm from the capillary, and the measurement was carried out after 1 min of irradiation. The modulation frequency was 100 kHz; the modulation amplitude was 0.2 mT; the microwave power was 10 mW; and the sweep time was 60 s.

2.2 Nitrate–TiO_2 composite samples

In our experiments, two nitrate salts – potassium nitrate (AR, Beijing Chemical Works Co., Ltd) or ammonium nitrate (AR, Beijing Chemical Works Co., Ltd) – were composited with pure TiO_2 ($\geq$ 99.5 %, Degussa AG) powder or TiO_2 (1 wt %) / SiO_2 mixed powder to prepare NO_3^-–TiO_2 or NO_3^-–TiO_2 (1 wt %) / SiO_2 samples; 250 mg TiO_2 was simply mixed in the nitrate solutions at the desired mass mixing ratio (with nitrate content of 4 wt %) to obtain a mash. The mash was dried at 90 °C and then ground carefully for 30 min. A series of samples with different amounts of nitrate were prepared, and diffuse reflectance Fourier transform infrared spectroscopy (DRIFTS) measurements were made to test their homogeneity. Figure S2 shows the DRIFTS spectra of these KNO_3–TiO_2 composites, of which the 1760 cm^{-1} peak is one of the typical vibrating peaks of nitrate (Aghazadeh, 2016; Maeda et al., 2011). The ratio value of the peak area from 1730–1790 cm^{-1} for 1 wt %, 4 wt %, 32 wt %, 80 wt % composited samples is 1 : 4.1 : 29.8 : 81.6, which is very close to that of theoretical value, proving that the samples were uniformly mixed. SiO_2 (AR, Xilong Scientific Co., Ltd.) with no optical activity was also chosen for comparison, and samples of KNO_3-SiO_2 and KNO_3–TiO_2 (1 wt %) / SiO_2 samples with a potassium nitrate content of 4 wt % were prepared. The blank 250 mg TiO_2 sample was solved in pure water, using the same procedure as mentioned above. Four wt % HNO_3–TiO_2 composite particles were prepared for comparison. Concentrated nitric acid (AR, Beijing Chemical Works Co., Ltd) was diluted to 1 M, and 250 mg TiO_2 was added to the nitric acid solution and stirred evenly. A layer of aluminum foil was used to cover the surface of the HNO_3–TiO_2 homogenate, which was then dried naturally in the room and then ground for use. We also selected Arizona Test Dust (ATD, Powder Technology Inc.), whose chemical composition and weight percentage were shown in Table S1, as a substitute of NO_3^- / TiO_2 to investigate the "photocatalytic renoxification" process of nitrate and the positive effect of HCHO.

2.3 Environmental chamber experiments

For the chamber operation, we completely evacuated the chamber after every experiment; we then cleaned the chamber walls with deionized water and dried them by flushing the chamber with ultra-zero air to remove any particles or gases that had collected on the chamber walls. The experiments carried out in the environmental chamber can be divided into two categories according to whether HCHO was involved or not. (1) No HCHO involvement in the reaction. The PVF bag was inflated by 260 L synthetic air, and then 75 mg particles were instantly sprayed into the chamber by a transient high-pressure airflow. As shown in Fig. S3, the particle number concentration of the KNO_3–TiO_2 or TiO_2 samples decreased rapidly owing to the wall effect, including the possible electrostatic adsorption of the particles by the environmental chamber. The size distributions of the KNO_3–TiO_2 and TiO_2 samples were similar, with both becoming stable after about 60 min. The peak number concentration was averaged between 3991 and 3886 particle cm^{-3} during the illumination period for the KNO_3–TiO_2 and TiO_2 samples, respectively, indicating that the repeatability of the introduction of particles into the chamber is good. This can be attributed to the strict cleaning of the chamber and the same operation of each batch experiment. (2) With the participation of HCHO. The PVF bag was inflated by 125 L synthetic air followed by the introduction of HCHO, and then the chamber was filled up with zero air to about 250 L. In order to know the HCHO adsorption before and after the particles' introduction, we conducted a conditional experiment in the dark. It can be seen from Fig. S4 that it took about 90 min for the concentration of HCHO to reach stability and be sustained. Then, 75 mg TiO_2 or NO_3^- / TiO_2 powders were introduced instantly, and the concentration of HCHO decreased upon the introduction. It took about 60 min for HCHO to reach its second adsorption equilibrium and for the concentration of HCHO to remain stable for several hours in the dark. Therefore, for the irradiation experiments, the particles were injected at 90 min after HCHO's introduction, and the lamps were turned on at 60 min after the particle's introduction.

To determine the background value of NO_x in the reaction system, four blank experiments were carried out under illumination without nitrate: "synthetic air", "synthetic air + TiO_2", "synthetic air + HCHO", and "synthetic air + HCHO + TiO_2". In the blank experiments of "synthetic air" and "synthetic air + TiO_2", the NO_x concentration remained stable during 180 min illumination, and the concentration change was no more than 0.5 ppb (Fig. S5a). Therefore, the environmental chamber, the synthetic air, and the surface of TiO_2 particles were thought to be relatively clean, and there was no generation and accumulation of NO_x under illumination. When HCHO was introduced into the environmental chamber, NO_x accumulated $\sim$ 2 ppb in 120 min with or without TiO_2 particles (Fig. S5b). Compared with the blank experiment results when there was no HCHO, NO_x might come from the generation process of HCHO (impurities in paraformaldehyde). However, considering the high concentration level of NO_x produced in the NO_3^-–TiO_2 system containing HCHO under the same conditions in this study (see later in Fig. 2), the NO_x generated in this blank experiment can be negligible.

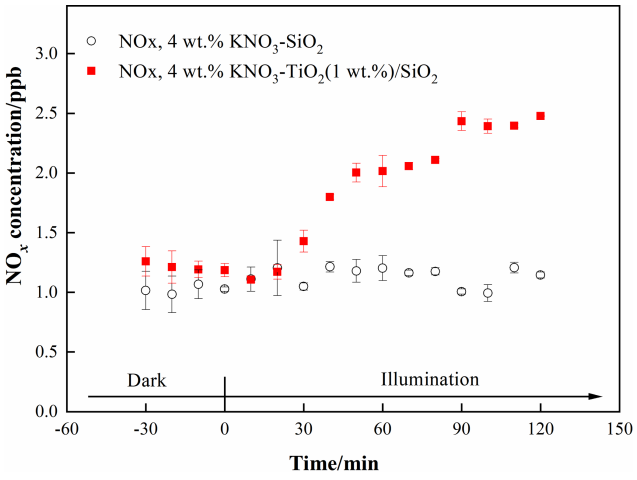

Figure 1. Effect of illumination on the release of NO_x from 4 wt % KNO_3-SiO_2 and 4 wt % KNO_3–TiO_2(1 wt %) / SiO_2 at 293 K and 0.8 % of relative humidity. 365 nm tube lamps were used during the illumination experiments.

3 Results and discussion

3.1 The positive effect of TiO_2 on the renoxification process

We investigated the photocatalytic role of TiO_2 on renoxification. The light source was two 365 nm tube lamps containing small amounts of 400–600 nm visible light; this setup was suitable for exciting TiO_2 and the photolysis of available nitrate radicals. Raw NO_x data measured in the chamber under dark and illuminated conditions for 4 wt % KNO_3-SiO_2 and 4 wt % KNO_3–TiO_2 (1 wt %) / SiO_2 are shown in Fig. 1. The ratio of 1 wt % TiO_2 to SiO_2 corresponds to their ratio in sand and dust particles. We observed no NO_x in the KNO_3-SiO_2 sample under darkness or illumination, indicating very weak direct photolysis of nitrate under our 365 nm tube-lamp illumination conditions. However, when the sample containing TiO_2 / SiO_2 was illuminated, NO_x continually accumulated in the chamber. This finding confirms that NO_x production arising from photodissociation of NO_3^- on TiO_2 /,SiO_2 was caused by the photocatalytic property of TiO_2 (i.e., photocatalytic renoxification) and was not due to the direct photolysis of NO_3^- (photolytic renoxification).

TiO_2 can be excited by UV illumination to generate electron-hole pairs, and the h^+ can react with adsorbed NO_3^- to produce NO_3• (Ndour et al., 2009). Thus, in the present study, NO_3• mainly absorbed visible light emitted from the tube lamps, which was subsequently photolyzed to NO_x through Eqs. (3) and (4) (Wayne et al., 1991), which explains why NO_x was observed in this study. Thus, we demonstrated that TiO_2 can be excited at illumination wavelengths of ∼ 365 nm, even when then content was very low, and that NO_x accumulated due to the production and further photolysis of NO_3•. However, the production rate of NO_x was very slow, reaching only 1.3 ppb during 90 min of illumination. This result may have been caused by the blocking effect of K^+ on NO_3^-. K^+ forms ion pairs with NO_3^-, and electrostatic repulsion between K^+ and h^+ prevents NO_3^- from combining with h^+ to generate NO_3• to a certain extent, thereby weakening the positive effect of TiO_2 on the renoxification of KNO_3 (Rosseler et al., 2013).

$$TiO_2 + h\upsilon(\lambda < 390\,\text{nm}) \rightarrow e^- + h^+. \quad (1)$$

$$NO_3^- + h^+ \rightarrow NO_3\bullet. \quad (2)$$

$$NO_3\bullet + h\upsilon(\lambda < 640\,\text{nm}) \rightarrow NO_2 + O\bullet. \quad (3)$$

$$NO_3\bullet + h\upsilon(585\,\text{nm} < \lambda < 640\,\text{nm}) \rightarrow NO + O_2. \quad (4)$$

3.2 The synergistic positive effect of TiO_2 and HCHO on the renoxification process

LED lamps with a wavelength range of 350–390 nm and no visible light were used to irradiate 4 wt % KNO_3–TiO_2 without generating NO_x (NO_2 and NO concentrations fluctuate within the error range of the instrument) (Fig. S5). TiO_2 can be excited under this range of irradiation, producing NO_3 radicals as discussed above. The lack of NO_x generation indicates that neither nitrate photolysis nor NO_3• photolysis occurred under 365 nm LED lamp illumination conditions. In addition, it has been shown that NO_3• photolysis only occurs in visible light (Aldener et al., 2006). Therefore, the LED lamp setup was used in subsequent experiments to exclude the direct photolysis of both KNO_3 and NO_3• but to allow the excitation of TiO_2. This approach allowed us to investigate the process of photocatalytic renoxification caused by HCHO in the presence of photogenerated NO_3•.

Atmospheric trace gases can undergo photocatalytic reactions on the surface of TiO_2 (Chen et al., 2012). As the illumination time increased, the concentration of HCHO showed a linear downward trend, which was found to fit zero-order reaction kinetics (Fig. S7). The zero-order reaction rate constants of HCHO on TiO_2 and 4 wt % KNO_3–TiO_2 particles were 9.1×10^{-3} and 1.4×10^{-2} ppm min^{-1}, respectively, which were much higher than that for gaseous HCHO photolysis (Shang et al., 2017). We suggested that the produced NO_3• contributed to the enhanced uptake of HCHO. In the following study, the effect of HCHO on the photocatalytic renoxification of NO_3^-–TiO_2 was explored.

The variation in NO_x concentrations within the chamber containing nitrate–TiO_2 particles with or without HCHO is shown in Fig. 2. For 4 wt % KNO_3–TiO_2 particles, the NO_x concentration began to increase upon irradiation in the presence of HCHO, reaching ∼ 3861 mmol normalized ppb (equivalent to 110 ppb) within 120 min. This result indicates that HCHO greatly promoted photocatalytic renoxification of KNO_3 on the surfaces of TiO_2 particles. This reaction process can be divided into two stages: a rapid increase within the first 60 min and a slower increase within the following 60 min, each consistent with zero-orde reaction kinetics. The slow stage is due to the photodegradation of HCHO on

KNO_3–TiO_2 aerosols, which led to a decrease in its concentration, gradually weakening the positive effect. NO_x is the sum of NO_2 and NO, both of which showed a two-stage concentration increase (Fig. S8). The NO_2 generation rate was nearly 6 times that of NO as compared to using the zero-order rate constant within 60 min (1.18 ppb min^{-1} NO_2, $R^2 = 0.96$; 0.19 ppb min^{-1} NO, $R^2 = 0.91$). This burst-like generation of NO_x can be ascribed to the reaction between generated NO_3• and HCHO via hydrogen abstraction to form adsorbed nitric acid (HNO_3(ads)) on TiO_2 particles. We measured the pH of water extracts in NO_3^-–TiO_2 systems with and without HCHO. It was found that the pH decreased by 1.7 % for KNO_3–TiO_2, suggesting the formation of acidic species such as HNO_3(ads) in this study. Based on the analysis of the absorption cross section of HNO_3 adsorbed on the fused silica surface, the HNO_3(ads) absorption spectrum has been reported to be red-shifted compared to HNO_3(g), extending from 350 to 365 nm, with a simultaneous cross-sectional increase (Du and Zhu, 2011). Therefore, HNO_3(ads) was subjected to photolysis to produce NO_2 and HONO (Eqs. 6–8) under the LED lamp used in this study. A previous study of HNO_3 photolysis on the surface of Pyrex glass showed that the ratio of the formation rates of photolysis products ($J_{NO_x}/J_{(NO_x+HONO)}$) was > 97 % at RH = 0 % (Zhou et al., 2003), suggesting that NO_x is the main gaseous product under dry conditions. Thus, the effect of HONO on product distribution and NO_x concentration was negligible in this study. Together, these results suggest that NO_3• and HCHO generate HNO_3(ads) on particle surfaces through hydrogen abstraction, which contributes to the substantial release of NO_x via photolysis. This photocatalytic renoxification via the NO_3^-–NO_3•–HNO_3–NO_x pathway is important considering the high abundance of hydrogen donor organics in the atmosphere.

$$NO_3\bullet + HCHO \rightarrow CHO\bullet + HNO_3(ads) \quad (5)$$

$$HNO_3(ads) + h\upsilon \rightarrow [HNO_3]^*(ads) \quad (6)$$

$$[HNO_3]^*(ads) \rightarrow HNO_2(ads) + O(^3P)(ads) \quad (7)$$

$$[HNO_3]^*(ads) \rightarrow NO_2(ads) + \bullet OH(ads) \quad (8)$$

To demonstrate the proposed HCHO mechanism and the photolysis contribution of HNO_3 to NO_x, we prepared an HNO_3–TiO_2 sample by directly dissolving TiO_2 into dilute nitric acid. The formation of NO_x on HNO_3–TiO_2 without HCHO under illumination was obvious and at a rate comparable with that on KNO_3–TiO_2 with HCHO (Fig. 2). The renoxification of HNO_3–TiO_2 particles was further enhanced following the introduction of HCHO. This is because HNO_3 dissociates on particle surfaces to generate NO_3^-, such that HNO_3 exists on TiO_2 as both HNO_3(ads) and NO_3^-(ads). Similarly, NO_3^-(ads) completed the NO_3^-–NO_3•–HNO_3–NO_x pathway, as described above, through the reaction process shown in Eqs. (2) to (8). The rates of NO_x production from HNO_3–TiO_2 particles with and without HCHO were similar for the first 60 min (Fig. 2), mainly due to the direct photolysis of partial HNO_3(ads). However, after 60 min, NO_x was generated rapidly in the presence of HCHO, perhaps due to the dominant photocatalytic renoxification of NO_3^-(ads). These findings indicate that HCHO converts NO_3^- on particle surfaces into HNO_3(ads) by reacting with NO_3•, and then HNO_3(ads) photolyzes at a faster rate to generate NO_x, allowing HCHO to enhance the formation of NO_x. Overall, the photocatalytic renoxification of NO_3^-–TiO_2 particles affects atmospheric oxidation and the nitrogen cycle, and the presence of HCHO further enhances this impact.

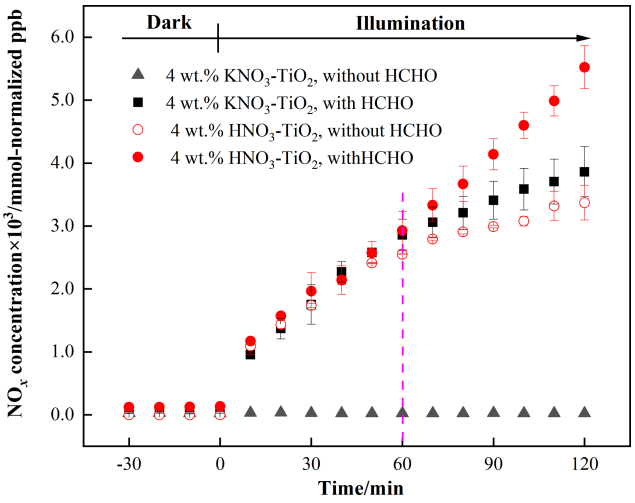

Figure 2. Effect of formaldehyde on the renoxification processes of different nitrate-doped particles at 293 K and 0.8 % of relative humidity; 365 nm LED lamps were used during the illumination experiment. The initial concentration of HCHO was about 9 ppm.

Photocatalytic renoxification reactions occur on the surfaces of mineral dust due to the presence of semiconductor oxides with photocatalytic activity such as TiO_2 (Ndour et al., 2009). In order to confirm this, we synthesized nitrate with inert SiO_2 as a comparison. It can be seen from Fig. S9 that no NO_2 formation was observed regardless of whether or not HCHO was present, indicating that photocatalytically active particle TiO_2 is critical to the photocatalytic renoxification process. Furthermore, a kind of commercial mineral dust ATD was selected to study the effects of HCHO on this process. We detected •OH in irradiated pure TiO_2 and ATD samples using the electron spin resonance (ESR) technique and found that, for ATD samples, the peak intensity of •OH generation was 40 % that of TiO_2 samples (Fig. S10). •OH originates in the reaction of h^+ with surface-adsorbed water (Ahmed et al., 2014). ATD contains semiconductor oxides such as TiO_2 and Fe_2O_3 and is thought to exhibit photocatalytic properties affecting the renoxification of nitrate. The NO_3^- content of ATD is 4×10^{17} molecules m^{-2}, which is ~ 0.25 wt % of the total mass (Huang et al., 2015; Park et al., 2017). The NO_x concentration changes observed in the envi-

ronmental chamber demonstrated that HCHO promoted the renoxification of ATD particles (Fig. S11). This result suggests that mineral dust containing photocatalytic semiconductor oxides such as TiO_2, Fe_2O_3, and ZnO can greatly promote the conversion of granular nitrate to NO_x in the presence of HCHO.

3.3 Influential factors on the photocatalytic renoxification process

3.3.1 The influence of nitrate type

As discussed above, HNO_3 and KNO_3 undergo different renoxification processes on the surface of TiO_2 under the same illumination conditions, suggesting that cations bound to NO_3^- significantly affect NO_x production. Different types of cations coexist with nitrate ions in atmospheric particulate matter, among which ammonium ions (NH_4^+) are important water-soluble ions that can be higher in content than K^+ in urban fine particulate matter (Zhou et al., 2016; Tang et al., 2021; Wang et al., 2021), especially in heavily polluted cities (Tian et al., 2020). Equal amounts of 4 wt % NH_4NO_3–TiO_2 particles were introduced into the chamber and illuminated under the same conditions. Similar to Fig. 2, millimole normalized ppb was used in order to compare the amount of NO_x released for different kinds of nitrate with the same percentage weight. It can be seen that HCHO had a much stronger positive effect on the release of NO_x over NH_4NO_3–TiO_2 particles (Fig. 3), which may be ascribed to NH_4^+. Combined with the results of NH_4NO_3–TiO_2 and KNO_3–TiO_2 particles, it seems that the affinity rather than electrostatic repulsion should be the primary effect of cations on the production of NO_x. On substrates without photocatalytic activity, such as SiO_2 and Al_2O_3, NH_4NO_3 cannot generate NO_x, such that NO_x production depends on the effect of TiO_2 (Ma et al., 2021). The h^+ generated by TiO_2 excitation reacts with adsorbed H_2O to produce •OH (Eq. 9), which gradually oxidizes NH_4^+ to NO_3^- (Eq. 10). In our previous study, we demonstrated that irradiated $(NH_4)_2SO_4$–TiO_2 samples had lower NH_4^+ and NO_3^- peaks (Shang et al., 2017). Therefore, more NO_3^- participated in the photocatalytic renoxification process via the NO_3^-–NO_3•–HNO_3–NO_x pathway to generate NO_x. Moreover, the results without HCHO are shown in Fig. S12. Both NH_4NO_3–TiO_2 particles and KNO_3–TiO_2 particles produced almost no NO_x, indicating the importance of HCHO for renoxification to occur. Due to the high content of NH_4NO_3 in atmospheric particulate matter, the positive effect of HCHO on the photocatalytic renoxification process may have some impact on the concentrations of NO_x and other atmospheric oxidants.

$$h^+ + H_2O \rightarrow \cdot OH. \quad (9)$$

$$\cdot OH + NH_4^+/NH_3 \rightarrow NO_2^- \rightarrow NO_3^-. \quad (10)$$

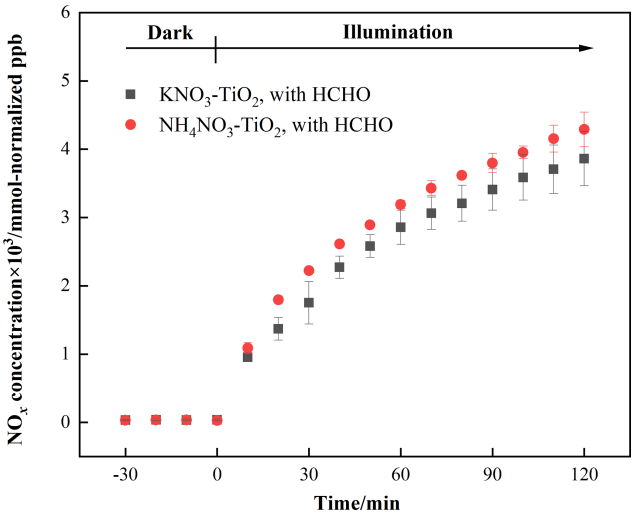

Figure 3. Effect of formaldehyde on the renoxification processes of 4 wt % NH_4NO_3–TiO_2 and 4 wt % KNO_3–TiO_2 particles at 293 K and 0.8 % of relative humidity; 365 nm LED lamps were used during the irradiation experiment. The initial concentration of HCHO was about 9 ppm.

3.3.2 The influence of relative humidity

Water on particle surfaces can participate directly in the heterogeneous reaction process. As shown in Eq. (9), H_2O can be captured by h^+ to generate •OH with strong oxidizability in photocatalytic reactions. The first-order photolysis rate constant of NO_3^- on TiO_2 particles decreases by an order of magnitude from $(5.7 \pm 0.1) \times 10^{-4}\ s^{-1}$ on dry surfaces to $(7.1 \pm 0.8) \times 10^{-5}\ s^{-1}$ when nitrate is coadsorbed with water above monolayer coverage (Ostaszewski et al., 2018). We explored the positive effect of HCHO on the NO_3^-–TiO_2 particle photocatalytic renoxification at different RH levels; the results are shown in Fig. 4a. For KNO_3–TiO_2 particles, the rate of NO_x production decreased as the RH of the environmental chamber increased, indicating that increased water content in the gas phase hindered photocatalytic renoxification for two reasons: H_2O competes with NO_3^- for h^+ on the surface of TiO_2 to generate •OH, reducing the generation of NO_3•, and competitive adsorption between H_2O and HCHO causes the generated •OH to compete with NO_3• for HCHO, hindering the formation of HNO_3(ads) on particle surfaces. Moreover, it is also possible that the loss of NO_x on the wall increases under high humidity conditions, resulting in a decrease in its concentration. This competitive process also occurs on the surface of NH_4NO_3–TiO_2 particles, but at RH = 70 %, the NO_x generation rate constant is slightly higher. The deliquescent humidity of NH_4NO_3 at 298 K is ∼62 %, such that NH_4NO_3 had already deliquesced at RH = 70 %, forming an NH_4^+/NH_3-NO_3^- liquid system on the particle surfaces. This quasi-liquid phase improved the dispersion of TiO_2 in NH_4NO_3, resulting in greater NO_x release. The deliquescent humidity of KNO_3–

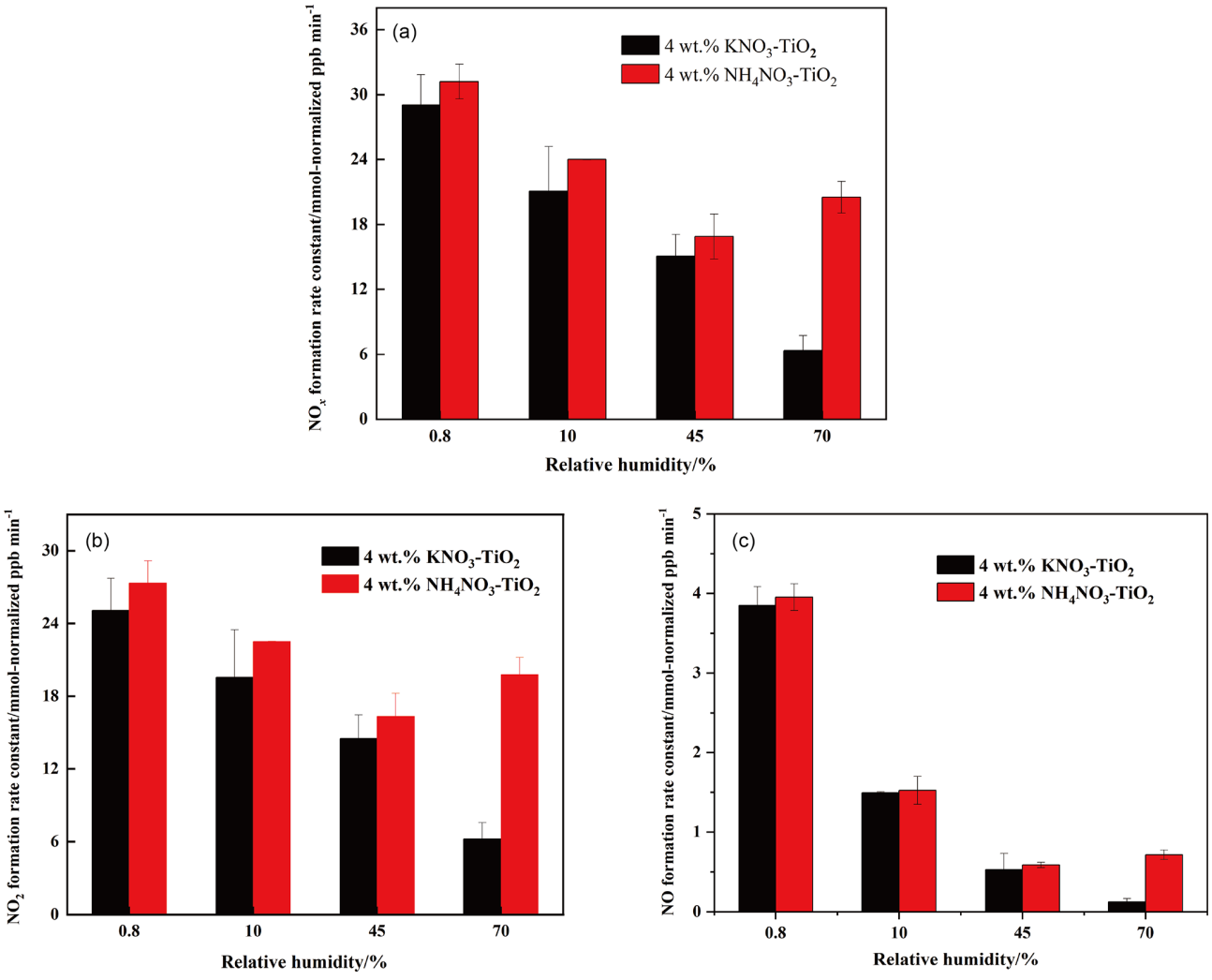

Figure 4. Effect of relative humidity on the release of NO_x **(a)**, NO_2 **(b)**, NO **(c)** over 4 wt % NH_4NO_3–TiO_2 and 4 wt % KNO_3–TiO_2 particles at 293 K; 365 nm LED lamps were used during the illumination experiment. The initial concentration of HCHO was about 9 ppm.

TiO_2 was > 90 % (2009), such that no phase change occurred at RH = 70 %, and the renoxification reaction rate retained a downward trend. In the presence of H_2O, in addition to the NO_3^--NO_3•-HNO_3 pathway observed in this study, there are a variety of HNO_3 generation paths, such as the hydrolysis of N_2O_5 via the NO_2-N_2O_5-HNO_3 pathway (Brown et al., 2005), the oxidation of NO_2 by •OH (Burkholder et al., 1993), and the reaction of NO_3• with H_2O (Schutze and Herrmann, 2005), all of which require further consideration and study.

The formation rates of NO and NO_2 are shown in Fig. 4b and c, respectively. NO_2 was the main product of surface HNO_3 photolysis. Under humid conditions, generated NO_2(ads) continued to react with H_2O adsorbed on the surface to form HONO(ads). HONO was desorbed from the surface and released into the gas phase (Zhou et al., 2003; Bao et al., 2018; Pandit et al., 2021), providing gaseous HONO to the reaction system. Because the NO_x concentration remained high, the effect of HONO on NO_x analyzer results was negligible (Shi et al., 2021). As NO_2 can form NO_2^- with e^-, a reverse reaction also occurred between NO_2^- and HONO in the presence of H_2O (Ma et al., 2021; Garcia et al., 2021). Therefore, the increase in H_2O increased the proportion of HONO in the nitrogen-containing products, such that the NO_x generation rate decreased as RH increased. Comparing Fig. 4b and c shows that, as RH increased, the NO production rate constant decreased more than that of NO_2. HONO and NO_2 generated by the photolysis of HNO_3(ads) decreased accordingly, i.e., the NO source decreased. However, generated NO_2 and NO underwent photocatalytic oxidation on the surface of TiO_2, and NO photodegradation was more significant under the same conditions (Hot et al., 2017). Generally, a certain amount of HONO will be generated during the reaction between HCHO and NO_3^-–TiO_2 particles

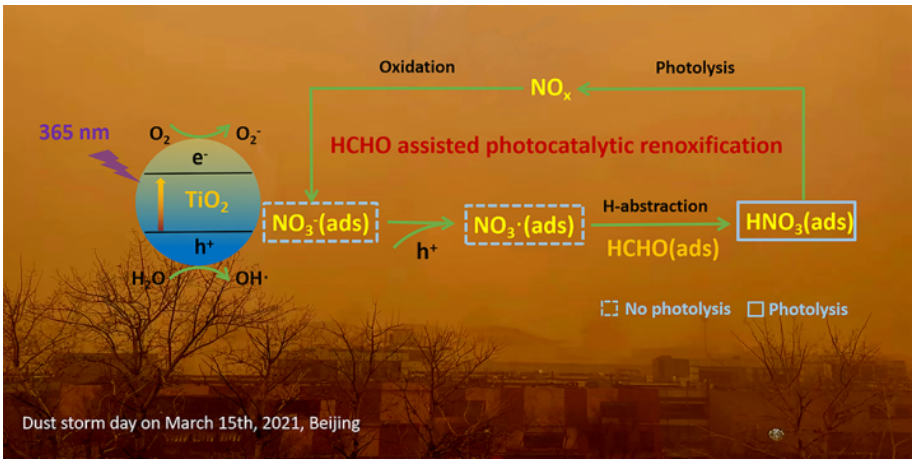

Figure 5. Positive role of HCHO on the photocatalytic renoxification of nitrate–TiO_2 composite particles via the NO_3^-–$NO_3\cdot$–HNO_3–NO_x pathway.

when RH is high, which affects the concentrations of atmospheric •OH, NO_x, and O_3. This process is more likely to occur in summer due to high RH and light intensity affecting atmospheric oxidation. In drier winters or dusty weather, when TiO_2 content is high, HCHO greatly promotes the photocatalytic renoxification of NO_3^-–TiO_2 particles, thereby releasing more NO_x into the atmosphere, affecting the global atmospheric nitrogen budget. Thus, regardless of the seasonal and regional changes, renoxification has significant practical importance.

3.3.3 The influence of initial HCHO concentrations

To explore whether HCHO promotes nitrate renoxification at natural concentration levels, we reduced the initial concentration of HCHO in the environmental chamber by a factor of 10 to ∼ 1.0 ppm. The positive effect of HCHO on the photocatalytic renoxification of KNO_3–TiO_2 particles was clearly weakened, with the NO_2 concentration first increasing and then decreasing, and the NO concentration remaining stable (Fig. S13). The HCHO concentration decreased due to its consumption during the reaction, making its positive effect decline quickly. The photocatalytic oxidation reaction between NO_x and photogenerated reactive oxygen species (ROS) on the TiO_2 surface further decreased the NO_x concentration. Photocatalytic oxidation of NO_x by ROS on TiO_2 particles occurred at an HCHO concentration of 9 ppm, but the positive effect of HCHO remained dominant. Thus, no decrease in NO_x concentration was observed within 120 min in our experiments.

The concentration of HCHO in the atmosphere is relatively low, with a balance between the photocatalytic oxidation decay of NO_x and the release of NO_x via photocatalytic renoxification. The mutual transformation between particulate NO_3^- and gaseous NO_x is more complex. The effect of low-concentration HCHO on the renoxification of NO_3^-–TiO_2 particles requires further investigation. However, many types of organics provide hydrogen atoms in the atmosphere, including alkanes (e.g., methane and n-hexane), aldehydes (e.g., acetaldehyde), alcohols (e.g., methanol and ethanol), and aromatic compounds (e.g., phenol) that react with $NO_3\cdot$ to produce nitric acid (Atkinson, 1991). These organics, together with HCHO, play similar positive roles in photocatalytic renoxification and, therefore, influence NO_x concentrations.

4 Atmospheric implications

Nitric acid and nitrate are not only the final sink of NO_x in the atmosphere but are also among its important sources. NO_x generated from nitrate through renoxification is easily overlooked. The renoxification of nitrate on the surface of TiO_2 particles can be divided into photolytic renoxification and photocatalytic renoxification. The photocatalytic performance of TiO_2 promotes the renoxification process, which explains the influence of semiconducting metal oxide components on atmospheric mineral particles during the renoxification of nitrate. Although most previous studies have focused on solid-phase nitrate renoxification, our exploration of the roles of HCHO in this study will allow us to examine complex real-world pollution scenarios, in which multiple atmospheric pollutants coexist, as well as the effects of organic pollutants on the renoxification process. Atmospheric HCHO is taken up at the surface of particulate matter, accounting for up to ∼ 50 % of its absorption (Li et al., 2014), such that the heterogeneous participation of HCHO during renoxification is important. This study is the first to report that HCHO has a positive effect on the photocatalytic renoxification of nitrate on TiO_2 particles via the NO_3^-–$NO_3\cdot$–HNO_3–NO_x pathway (Fig. 5), further increasing the release of NO_x and other nitrogen-containing active species, which

in turn affects the photochemical cycle of HO_x radicals in the atmosphere and the formation of important atmospheric oxidants such as O_3. Although the response to the real situation will be biased in the case of high concentrations of HCHO, as in our experiment, the results of this study illustrate a possible way in which HCHO influences nitrate renoxification in the atmosphere. Factors such as particulate matter composition, RH, and initial HCHO concentration all influence the positive effect of HCHO; notably, H_2O competes with NO_3^- for photogenerated holes. Based on these findings, two balance systems should be explored in depth: the influence of RH on the generation rates of HONO and NO_x, as water increases the proportion of HONO in nitrogen-containing products; and the balance between the photocatalytic degradation of generated NO_x on TiO_2 particles and the positive effect of HCHO on NO_x generation at low HCHO concentrations.

Based on our results, we conclude that, in photochemical processes on the surfaces of particles containing semiconductor oxides, with the participation of hydrogen donor organics, a significant synergistic photocatalytic renoxification enhancement effect could alter the composition of surface nitrogenous species via the NO_3^-–NO_3•–HNO_3–NO_x pathway, thereby affecting atmospheric oxidation and nitrogen cycling. The positive effect of HCHO can be extended from TiO_2 in this study to other components of mineral dust, such as Fe_2O_3 and ZnO with photocatalytic activity, which may have practical applications. Our proposed reaction mechanism by which HCHO promotes photocatalytic renoxification could improve existing atmospheric chemistry models and reduce discrepancies between model simulations and field observations.

Data availability. All data are available upon request from the corresponding authors: shangjing@pku.edu.cn.

Supplement. Detailed information of Figs. S1–S13 (which include the spectra of the lamps, size distribution of 4 wt % KNO_3–TiO_2 and TiO_2 particles, changes in HCHO concentrations in the environmental chamber, changes in NO_x concentrations under different reaction conditions, photodegradation curve of HCHO, and ESR spectra of TiO_2 and ATD particles) and Table S1 (which demonstrates ATD chemical composition). The supplement related to this article is available online at: https://doi.org/10.5194/acp-22-11347-2022-supplement.

Author contributions. YL and JS prepared the paper with contributions from other co-authors. JS and XW designed the experiments and carried them out. YL, XW and WX prepared the supplement. YL, JS, MS and CY discussed the results. JS and YL revised the paper.

Competing interests. The contact author has declared that none of the authors has any competing interests.

Disclaimer. Publisher's note: Copernicus Publications remains neutral with regard to jurisdictional claims in published maps and institutional affiliations.

Acknowledgements. The authors are grateful for the financial support provided by National Natural Science Foundation of China (nos. 21876003, 41961134034 and 21277004), the Second Tibetan Plateau Scientific Expedition and Research (no. 2019QZKK0607).

Financial support. This research has been supported by the National Natural Science Foundation of China (grant nos. 21876003, 41961134034, and 21277004) and the Second Tibetan Plateau Scientific Expedition and Research (grant no. 2019QZKK0607).

Review statement. This paper was edited by Ryan Sullivan and reviewed by three anonymous referees.

References

Aghazadeh, M.: Preparation of Gd_2O_3 Ultrafine Nanoparticles by Pulse Electrodeposition Followed by Heat-treatment Method, Journal of Ultrafine Grained and Nanostructured Materials, 49, 80–86, https://doi.org/10.7508/jufgnsm.2016.02.04, 2016.

Ahmed, A. Y., Kandiel, T. A., Ivanova, I., and Bahnemann, D.: Photocatalytic and photoelectrochemical oxidation mechanisms of methanol on TiO_2 in aqueous solution, Appl. Surf. Sci., 319, 44–49, https://doi.org/10.1016/j.apsusc.2014.07.134, 2014.

Aldener, M., Brown, S. S., Stark, H., Williams, E. J., Lerner, B. M., Kuster, W. C., Goldan, P. D., Quinn, P. K., Bates, T. S., Fehsenfeld, F. C., and Ravishankara, A. R.: Reactivity and loss mechanisms of NO_3 and N_2O_5 in a polluted marine environment: Results from in situ measurements during New England Air Quality Study 2002, J. Geophys. Res.-Atmos., 111, D23S73, https://doi.org/10.1029/2006jd007252, 2006.

Alexander, B., Sherwen, T., Holmes, C. D., Fisher, J. A., Chen, Q., Evans, M. J., and Kasibhatla, P.: Global inorganic nitrate production mechanisms: comparison of a global model with nitrate isotope observations, Atmos. Chem. Phys., 20, 3859–3877, https://doi.org/10.5194/acp-20-3859-2020, 2020.

Atkinson, R.: Kinetics and mechanisms of the gas-phase reactions of the NO_3 radical with organic-comounds, J. Phys Chem. Ref. Data, 20, 459–507, https://doi.org/10.1063/1.555887, 1991.

Baergen, A. M. and Donaldson, D. J.: Photochemical Renoxification of Nitric Acid on Real Urban Grime, Environ. Sci. Technol., 47, 815–820, https://doi.org/10.1021/es3037862, 2013.

Bao, F., Li, M., Zhang, Y., Chen, C., and Zhao, J.: Photochemical Aging of Beijing Urban $PM_{2.5}$: HONO Production, Environ. Sci. Technol., 52, 6309–6316, https://doi.org/10.1021/acs.est.8b00538, 2018.

Bao, F., Jiang, H., Zhang, Y., Li, M., Ye, C., Wang, W., Ge, M., Chen, C., and Zhao, J.: The Key Role of Sulfate in the Photo-

chemical Renoxification on Real $PM_{2.5}$, Environ. Sci. Technol., 54, 3121–3128, https://doi.org/10.1021/acs.est.9b06764, 2020.

Bedjanian, Y. and El Zein, A.: Interaction of NO_2 with TiO_2 Surface Under UV Irradiation: Products Study, J. Phys. Chem. A, 116, 1758–1764, https://doi.org/10.1021/jp210078b, 2012.

Brown, S. S., Osthoff, H. D., Stark, H., Dube, W. P., Ryerson, T. B., Warneke, C., de Gouw, J. A., Wollny, A. G., Parrish, D. D., Fehsenfeld, F. C., and Ravishankara, A. R.: Aircraft observations of daytime NO_3 and N_2O_5 and their implications for tropospheric chemistry, J. Photoch. Photobio. A, 176, 270–278, https://doi.org/10.1016/j.jphotochem.2005.10.004, 2005.

Burkholder, J. B., Talukdar, R. K., Ravishankara, A. R., and Solomon, S.: Temperature-dependence of the HNO_3 UV absorption cross-sections, J. Geophys. Res.-Atmos., 98, 22937–22948, https://doi.org/10.1029/93jd02178, 1993.

Chen, H., Nanayakkara, C. E., and Grassian, V. H.: Titanium Dioxide Photocatalysis in Atmospheric Chemistry, Chem. Rev., 112, 5919–5948, https://doi.org/10.1021/cr3002092, 2012.

Deng, J. J., Wang, T. J., Liu, L., and Jiang, F.: Modeling heterogeneous chemical processes on aerosol surface, Particuology, 8, 308–318, https://doi.org/10.1016/j.partic.2009.12.003, 2010.

Dentener, F. J. and Crutzen, P. J.: Reaction of N_2O_5 on tropospheric aerosols-impact on the global distributions od NO_x, O_3, and OH, J. Geophys. Res.-Atmos., 98, 7149–7163, https://doi.org/10.1029/92jd02979, 1993.

Du, J. and Zhu, L.: Quantification of the absorption cross sections of surface-adsorbed nitric acid in the 335-365 nm region by Brewster angle cavity ring-down spectroscopy, Chem. Phys. Lett., 511, 213–218, https://doi.org/10.1016/j.cplett.2011.06.062, 2011.

Finlayson-Pitts, B. J. and Pitts, J. J. N.: Chemistry of the Upper and Lower Atmosphere: Theory, Experiments and Applications, Academic Press, https://doi.org/10.1016/B978-012257060-5/50000-9, 1999.

Garcia, S. L. M., Pandit, S., Navea, J. G., and Grassian, V. H.: Nitrous Acid (HONO) Formation from the Irradiation of Aqueous Nitrate Solutions in the Presence of Marine Chromophoric Dissolved Organic Matter: Comparison to Other Organic Photosensitizers, Acs Earth and Space Chemistry, 5, 3056–3064, https://doi.org/10.1021/acsearthspacechem.1c00292, 2021.

George, C., Ammann, M., D'Anna, B., Donaldson, D. J., and Nizkorodov, S. A.: Heterogeneous Photochemistry in the Atmosphere, Chem. Rev., 115, 4218–4258, https://doi.org/10.1021/cr500648z, 2015.

Goodman, A. L., Bernard, E. T., and Grassian, V. H.: Spectroscopic study of nitric acid and water adsorption on oxide particles: Enhanced nitric acid uptake kinetics in the presence of adsorbed water, J. Phys. Chem. A, 105, 6443–6457, https://doi.org/10.1021/jp003722l, 2001.

Harris, G. W., Carter, W. P. L., Winer, A. M., Pitts, J. N., Platt, U., and Perner, D.: Observations of nitrous-acid in the los-angeles atmosphere and implications for predictions of ozone precursor relationships, Environ. Sci. Technol., 16, 414–419, https://doi.org/10.1021/es00101a009, 1982.

Hot, J., Martinez, T., Wayser, B., Ringot, E., and Bertron, A.: Photocatalytic degradation of NO / NO_2 gas injected into a 10 m^3 experimental chamber, Environ. Sci. Poll. R., 24, 12562–12570, https://doi.org/10.1007/s11356-016-7701-2, 2017.

Huang, L., Zhao, Y., Li, H., and Chen, Z.: Kinetics of Heterogeneous Reaction of Sulfur Dioxide on Authentic Mineral Dust: Effects of Relative Humidity and Hydrogen Peroxide, Environ. Sci. Technol., 49, 10797–10805, https://doi.org/10.1021/acs.est.5b03930, 2015.

Kasibhatla, P., Sherwen, T., Evans, M. J., Carpenter, L. J., Reed, C., Alexander, B., Chen, Q., Sulprizio, M. P., Lee, J. D., Read, K. A., Bloss, W., Crilley, L. R., Keene, W. C., Pszenny, A. A. P., and Hodzic, A.: Global impact of nitrate photolysis in sea-salt aerosol on NO_x, OH, and O_3 in the marine boundary layer, Atmos. Chem. Phys., 18, 11185–11203, https://doi.org/10.5194/acp-18-11185-2018, 2018.

Kim, W.-H., Song, J.-M., Ko, H.-J., Kim, J. S., Lee, J. H., and Kang, C.-H.: Comparison of Chemical Compositions of Size-segregated Atmospheric Aerosols between Asian Dust and Non-Asian Dust Periods at Background Area of Korea, B. Kor. Chem. Soc., 33, 3651–3656, https://doi.org/10.5012/bkcs.2012.33.11.3651, 2012.

Lee, J. D., Moller, S. J., Read, K. A., Lewis, A. C., Mendes, L., and Carpenter, L. J.: Year-round measurements of nitrogen oxides and ozone in the tropical North Atlantic marine boundary layer, J. Geophys. Res.-Atmos., 114, D21302, https://doi.org/10.1029/2009jd011878, 2009.

Lesko, D. M. B., Coddens, E. M., Swomley, H. D., Welch, R. M., Borgatta, J., and Navea, J. G.: Photochemistry of nitrate chemisorbed on various metal oxide surfaces, Phys. Chem. Chem. Phys., 17, 20775–20785, https://doi.org/10.1039/c5cp02903a, 2015.

Li, X., Rohrer, F., Brauers, T., Hofzumahaus, A., Lu, K., Shao, M., Zhang, Y. H., and Wahner, A.: Modeling of HCHO and CHOCHO at a semi-rural site in southern China during the PRIDE-PRD2006 campaign, Atmos. Chem. Phys., 14, 12291–12305, https://doi.org/10.5194/acp-14-12291-2014, 2014.

Linsebigler, A. L., Lu, G. Q., and Yates, J. T.: Photocatalysis on TiO_2 surfaces-principles, mechanisms, and selected results, Chem. Rev., 95, 735–758, https://doi.org/10.1021/cr00035a013, 1995.

Liu, W., Wang, Y. H., Russell, A., and Edgerton, E. S.: Atmospheric aerosol over two urban-rural pairs in the southeastern United States: Chemical composition and possible sources, Atmos. Environ., 39, 4453–4470, https://doi.org/10.1016/j.atmosenv.2005.03.048, 2005.

Ma, Q., Zhong, C., Ma, J., Ye, C., Zhao, Y., Liu, Y., Zhang, P., Chen, T., Liu, C., Chu, B., and He, H.: Comprehensive Study about the Photolysis of Nitrates on Mineral Oxides, Environ. Sci. Technol., 55, 8604–8612, https://doi.org/10.1021/acs.est.1c02182, 2021.

Maeda, N., Urakawa, A., Sharma, R., and Baiker, A.: Influence of Ba precursor on structural and catalytic properties of Pt-Ba / alumina NO_x storage-reduction catalyst, Appl. Catal. B-Environ., 103, 154–162, https://doi.org/10.1016/j.apcatb.2011.01.022, 2011.

Monge, M. E., D"Anna, B., and George, C.: Nitrogen dioxide removal and nitrous acid formation on titanium oxide surfaces–an air quality remediation process?, Phys. Chem. Chem. Phys., 12, 8991–8998, https://doi.org/10.1039/b925785c, 2010.

Ndour, M., Conchon, P., D'Anna, B., Ka, O., and George, C.: Photochemistry of mineral dust surface as a potential atmospheric renoxification process, Geophys. Res. Lett., 36, L05816, https://doi.org/10.1029/2008gl036662, 2009.

Ninneman, M., Lu, S., Zhou, X. L., and Schwab, J.: On the Importance of Surface-Enhanced Renoxification as an Oxides of Nitrogen Source in Rural and Urban New York State, Acs Earth and Space Chemistry, 4, 1985–1992, https://doi.org/10.1021/acsearthspacechem.0c00185, 2020.

Ostaszewski, C. J., Stuart, N. M., Lesko, D. M. B., Kim, D., Lueckheide, M. J., and Navea, J. G.: Effects of Coadsorbed Water on the Heterogeneous Photochemistry of Nitrates Adsorbed on TiO_2, J. Phys. Chem. A, 122, 6360–6371, https://doi.org/10.1021/acs.jpca.8b04979, 2018.

Pandit, S., Garcia, S. L. M., and Grassian, V. H.: HONO Production from Gypsum Surfaces Following Exposure to NO_2 and HNO_3: Roles of Relative Humidity and Light Source, Environ. Sci. Technol., 55, 9761–9772, https://doi.org/10.1021/acs.est.1c01359, 2021.

Park, J., Jang, M., and Yu, Z. C.: Heterogeneous Photo-oxidation of SO_2 in the Presence of Two Different Mineral Dust Particles: Gobi and Arizona Dust, Environ. Sci. Technol., 51, 9605–9613, https://doi.org/10.1021/acs.est.7b00588, 2017.

Platt, U., Perner, D., Harris, G. W., Winer, A. M., and Pitts, J. N.: Observations of nitrous-acid in an urban atmosphere by differential optical-absorption, Nature, 285, 312–314, https://doi.org/10.1038/285312a0, 1980.

Read, K. A., Mahajan, A. S., Carpenter, L. J., Evans, M. J., Faria, B. V. E., Heard, D. E., Hopkins, J. R., Lee, J. D., Moller, S. J., Lewis, A. C., Mendes, L., McQuaid, J. B., Oetjen, H., Saiz-Lopez, A., Pilling, M. J., and Plane, J. M. C.: Extensive halogen-mediated ozone destruction over the tropical Atlantic Ocean, Nature, 453, 1232–1235, https://doi.org/10.1038/nature07035, 2008.

Reed, C., Evans, M. J., Crilley, L. R., Bloss, W. J., Sherwen, T., Read, K. A., Lee, J. D., and Carpenter, L. J.: Evidence for renoxification in the tropical marine boundary layer, Atmos. Chem. Phys., 17, 4081–4092, https://doi.org/10.5194/acp-17-4081-2017, 2017.

Romer, P. S., Wooldridge, P. J., Crounse, J. D., Kim, M. J., Wennberg, P. O., Dibb, J. E., Scheuer, E., Blake, D. R., Meinardi, S., Brosius, A. L., Thames, A. B., Miller, D. O., Brune, W. H., Hall, S. R., Ryerson, T. B., and Cohen, R. C.: Constraints on Aerosol Nitrate Photolysis as a Potential Source of HONO and NO_x, Environ. Sci. Technol., 52, 13738–13746, https://doi.org/10.1021/acs.est.8b03861, 2018.

Rosseler, O., Sleiman, M., Nahuel Montesinos, V., Shavorskiy, A., Keller, V., Keller, N., Litter, M. I., Bluhm, H., Salmeron, M., and Destaillats, H.: Chemistry of NO_x on TiO_2 Surfaces Studied by Ambient Pressure XPS: Products, Effect of UV Irradiation, Water, and Coadsorbed K^+, J. Phys. Chem. Lett., 4, 536–541, https://doi.org/10.1021/jz302119g, 2013.

Salthammer, T.: Formaldehyde sources, formaldehyde concentrations and air exchange rates in European housings, Build. Environ., 150, 219–232, https://doi.org/10.1016/j.buildenv.2018.12.042, 2019.

Schuttlefield, J., Rubasinghege, G., El-Maazawi, M., Bone, J., and Grassian, V. H.: Photochemistry of adsorbed nitrate, J. Am. Chem. Soc., 130, 12210–12211, https://doi.org/10.1021/ja802342m, 2008.

Schutze, M. and Herrmann, H.: Uptake of the NO_3 radical on aqueous surfaces, J. Atmos. Chem., 52, 1–18, https://doi.org/10.1007/s10874-005-6153-8, 2005.

Schwartz-Narbonne, H., Jones, S. H., and Donaldson, D. J.: Indoor Lighting Releases Gas Phase Nitrogen Oxides from Indoor Painted Surfaces, Environ. Sci. Tech. Let., 6, 92–97, https://doi.org/10.1021/acs.estlett.8b00685, 2019.

Seltzer, K. M., Vizuete, W., and Henderson, B. H.: Evaluation of updated nitric acid chemistry on ozone precursors and radiative effects, Atmos. Chem. Phys., 15, 5973–5986, https://doi.org/10.5194/acp-15-5973-2015, 2015.

Shang, J., Xu, W. W., Ye, C. X., George, C., and Zhu, T.: Synergistic effect of nitrate-doped TiO_2 aerosols on the fast photochemical oxidation of formaldehyde, Sci. Rep.-UK, 7, 1161, https://doi.org/10.1038/s41598-017-01396-x, 2017.

Shi, Q., Tao, Y., Krechmer, J. E., Heald, C. L., Murphy, J. G., Kroll, J. H., and Ye, Q.: Laboratory Investigation of Renoxification from the Photolysis of Inorganic Particulate Nitrate, Environ. Sci. Technol., 55, 854–861, https://doi.org/10.1021/acs.est.0c06049, 2021.

Stemmler, K., Ammann, M., Donders, C., Kleffmann, J., and George, C.: Photosensitized reduction of nitrogen dioxide on humic acid as a source of nitrous acid, Nature, 440, 195–198, https://doi.org/10.1038/nature04603, 2006.

Sun, Y. L., Zhuang, G. S., Wang, Y., Zhao, X. J., Li, J., Wang, Z. F., and An, Z. S.: Chemical composition of dust storms in Beijing and implications for the mixing of mineral aerosol with pollution aerosol on the pathway, J. Geophys. Res.-Atmos., 110, D24209, https://doi.org/10.1029/2005jd006054, 2005.

Tang, M., Liu, Y., He, J., Wang, Z., Wu, Z., and Ji, D.: In situ continuous hourly observations of wintertime nitrate, sulfate and ammonium in a megacity in the North China plain from 2014 to 2019: Temporal variation, chemical formation and regional transport, Chemosphere, 262, 127745, https://doi.org/10.1016/j.chemosphere.2020.127745, 2021.

Tian, S. S., Liu, Y. Y., Wang, J., Wang, J., Hou, L. J., Lv, B., Wang, X. H., Zhao, X. Y., Yang, W., Geng, C. M., Han, B., and Bai, Z. P.: Chemical Compositions and Source Analysis of $PM_{2.5}$ during Autumn and Winter in a Heavily Polluted City in China, Atmosphere, 11, 336, https://doi.org/10.3390/atmos11040336, 2020.

Verbruggen, S. W.: TiO_2 photocatalysis for the degradation of pollutants in gas phase: From morphological design to plasmonic enhancement, J. Photoch. Photobio. C, 24, 64–82, https://doi.org/10.1016/j.jphotochemrev.2015.07.001, 2015.

Wang, H., Miao, Q., Shen, L., Yang, Q., Wu, Y., Wei, H., Yin, Y., Zhao, T., Zhu, B., and Lu, W.: Characterization of the aerosol chemical composition during the COVID-19 lockdown period in Suzhou in the Yangtze River Delta, China, J. Environ. Sci.-China, 102, 110–122, https://doi.org/10.1016/j.jes.2020.09.019, 2021.

Wayne, R. P., Barnes, I., Biggs, P., Burrows, J. P., Canosamas, C. E., Hjorth, J., Lebras, G., Moortgat, G. K., Perner, D., Poulet, G., Restelli, G., and Sidebottom, H.: The nitrate radical-physics, chemistry, and the atmosphere, Atmos. Environ. A-Gen., 25, 1–203, https://doi.org/10.1016/0960-1686(91)90192-a, 1991.

Wilbourn, J., Heseltine, E., and Moller, H.: IARC Evaluates Wood dust and formaldehyde, Scand. J. Work Env. Hea., 21, 229–232, https://doi.org/10.5271/sjweh.1368, 1995.

Yang, F., Tan, J., Zhao, Q., Du, Z., He, K., Ma, Y., Duan, F., Chen, G., and Zhao, Q.: Characteristics of $PM_{2.5}$ speciation in representative megacities and across China, Atmos. Chem. Phys., 11, 5207–5219, https://doi.org/10.5194/acp-11-5207-2011, 2011.

Ye, C., Gao, H., Zhang, N., and Zhou, X.: Photolysis of Nitric Acid and Nitrate on Natural and Artificial Surfaces, Environ. Sci. Technol., 50, 3530–3536, https://doi.org/10.1021/acs.est.5b05032, 2016a.

Ye, C., Zhou, X., Pu, D., Stutz, J., Festa, J., Spolaor, M., Tsai, C., Cantrell, C., Mauldin, R. L., III, Campos, T., Weinheimer, A., Hornbrook, R. S., Apel, E. C., Guenther, A., Kaser, L., Yuan, B., Karl, T., Haggerty, J., Hall, S., Ullmann, K., Smith, J. N., Ortega, J., and Knote, C.: Rapid cycling of reactive nitrogen in the marine boundary layer, Nature, 532, 489–491, https://doi.org/10.1038/nature17195, 2016b.

Ye, C., Zhang, N., Gao, H., and Zhou, X.: Photolysis of Particulate Nitrate as a Source of HONO and NO_x, Environ. Sci. Technol., 51, 6849–6856, https://doi.org/10.1021/acs.est.7b00387, 2017.

Zhou, J. B., Xing, Z. Y., Deng, J. J., and Du, K.: Characterizing and sourcing ambient $PM_{2.5}$ over key emission regions in China I: Water-soluble ions and carbonaceous fractions, Atmos. Environ., 135, 20–30, https://doi.org/10.1016/j.atmosenv.2016.03.054, 2016.

Zhou, X. L., Gao, H. L., He, Y., Huang, G., Bertman, S. B., Civerolo, K., and Schwab, J.: Nitric acid photolysis on surfaces in low-NO_x environments: Significant atmospheric implications, Geophys. Res. Lett., 30, 2217, https://doi.org/10.1029/2003gl018620, 2003.